

Investigation on polyethersulfone membranes modified with Fe₃O₄–trisodium citrate nanoparticles

Kacper Szymański^{a,*}, Paulina Sienkiewicz^a, Dominika Darowna^a, Manu Jose^a,
Karolina Szymańska^b, Sylwia Mozia^a

^aFaculty of Chemical Technology and Engineering, Institute of Inorganic Chemical Technology and Environment Engineering, West Pomeranian University of Technology, Szczecin, Pułaskiego 10, 70-322 Szczecin, Poland, email: kacper.szymanski@zut.edu.pl (K. Szymański)

^bNanomaterials Physicochemistry Department, West Pomeranian University of Technology, Szczecin, Piastów 45, 70-311 Szczecin, Poland

Received 21 April 2018; Accepted 25 June 2018

ABSTRACT

Polyethersulfone (PES) ultrafiltration (UF) membranes modified with nanocomposite Fe₃O₄–trisodium citrate (C₆H₅Na₃O₇·2H₂O) nanoparticles (FeTCNPs) were prepared via the wet phase inversion method. The casting solution contained 15 wt% of PES and 1, 2, or 4 wt% of FeTCNPs in relation to polymer. *N,N*-Dimethylformamide was applied as a solvent. The investigations were focused on the influence of the nanomaterial concentration in the membrane matrix on the physicochemical and transport properties of the fabricated membranes as well as their proneness to fouling. Membranes were characterized using scanning electron microscopy and atomic force microscopy. The influence of the modification on membranes hydrophilicity was determined based on water contact angle values. It was found that the pure water flux in case of the membrane containing 2 wt% of FeTCNPs was higher for ca. 12% compared with that measured for the unmodified membrane. Moreover, the permeate flux decline during UF of bovine serum albumin solution was less severe in case of the membranes modified with 1 and 2 wt% of FeTCNPs than in the absence of NPs in membrane matrix.

Keywords: Modified membrane; Polyethersulfone; Fouling; Nanoparticles; Fe₃O₄–trisodium citrate

1. Introduction

Polyethersulfone (PES) is a polymer widely used for preparation of ultrafiltration (UF) and microfiltration membranes applied for water and wastewater treatment and reuse due to its excellent chemical, thermal, and mechanical stability [1–3]. However, due to a relatively low hydrophilicity of this polymer, the membranes made of PES suffer from fouling, which is an undesired phenomenon in membrane processes [1,4]. Fouling occurs when organic or inorganic substances present in a feed are deposited on a membrane surface and/or within membrane pores. Under such conditions, microorganisms can additionally form a biofilm leading to the occurrence of the so-called biofouling [4].

Fouling causes a decrease of permeate flux and leads to a shortening of a membrane lifetime. In many cases the pores blockage is irreversible and the recovery of initial productivity of a membrane is impossible [4]. Hence, various membrane modifications aiming to mitigate fouling have been proposed. Among numerous attempts, fabrication of membranes by introduction of different fillers into the polymer matrix, aimed at the enhancement of membrane hydrophilicity is one of the main directions under development [5,6]. Recently nanotechnology has created new possibilities of membrane fabrication based on the application of nanomaterials. The most often used nanomodifiers of PES membranes are multi- or single-walled carbon nanotubes, halloysite nanotubes, TiO₂ nanoparticles (NPs), silica (SiO₂), Al₂O₃ or copper and silver NPs. These nanomaterials have

* Corresponding author.

generally been used to improve anti(bio)fouling performance via a good dispersion within a membrane matrix and increase of its hydrophilicity [6].

Recently, the attention of researchers has turned to the modification of polymeric membranes with Fe_3O_4 NPs. These nanomodifiers characterize with excellent thermal and chemical stability and good magnetic properties [7], whereas, membranes modified with Fe_3O_4 -NPs have been reported to exhibit higher permeate flux, improved separation properties, and superior fouling resistance compared with neat polymeric membranes used in UF [8,9]. Huang et al. [7] proposed a novel nanocomposite membrane made of polyvinylidene fluoride with addition of Fe_3O_4 NPs, exhibiting enhanced pure water flux (PWF), higher rejection, and better fouling resistance as well as good compaction resistance ability. Another authors [10] applied $\alpha\text{-Fe}_2\text{O}_3$ NPs synthesized by sol-gel method to enhance salt rejection by polysulfone (PSF) membrane. They found a positive effect of $\alpha\text{-Fe}_2\text{O}_3$ NPs on membrane properties such as permeability, hydrophilicity, porosity, and pore size. The PWF increased more than three times compared with the neat PSF membrane. In another work [11] Fe_3O_4 /PSF nanocomposite membranes were synthesized via three different methods, namely: blending with polymeric matrices, deposition by photopolymerization, and deposition by interfacial polymerization. The research revealed that the addition of the NPs to all of membranes led to an increase of permeate flux due to the improvement of surface hydrophilicity and contributed to the enhancement of separation properties. Mukherjee [12–14] indicated that the incorporation of iron oxide NPs into the polyacrylonitrile membrane could be effective in limitation of the microbial contamination of water. Based on the subject literature, it can be seen that a majority of publications on polymeric membranes modified with iron oxide NPs refer to the determination of the effectiveness of removal of metals, for example, lead, copper, zinc, cadmium, nickel, and chromium [15–21], as well as dyes [22,23] from water.

In most of literature reports, the enhancement of anti-fouling properties of UF, nanofiltration, and reverse osmosis membranes modified with iron oxide NPs is attributed to their higher hydrophilicity and porosity [10,16,20,22,24–27]. However, some papers reveal utterly different results, namely the permeation of pure water through the nanocomposite membranes decrease as a result of pore blockage by accumulated iron oxide NPs [12,18]. The above obstacle can possibly be overcome by application of iron oxide NPs modified by materials, which increase their hydrophilicity. It was reported [17] that a membrane fabricated from a casting dope containing 18 wt% PES, 1 wt% polyvinylpyrrolidone, and *N,N*-dimethylacetamide, modified with 0.01%–1% of Fe_3O_4 NPs covered with citrate groups exhibited an improvement of hydrophilicity and water flux as well as high efficiency of Cu(II) removal [17]. Trisodium citrate was chosen due to its anticoagulation properties.

In this work the investigations were focused on the determination of the influence of the amount of iron oxide NPs modified with trisodium citrate (FeTCNPs) on the physicochemical characteristics, water permeability, and antifouling properties of the UF PES membranes. The casting dope was prepared using PES (15 wt%) dissolved in *N,N*-dimethylformamide (DMF). The concentration of

FeTCNPs was in the range of 1–4 wt% in relation to polymer. Membranes were characterized using microscopic techniques, that is, scanning electron microscopy (SEM) and atomic force microscopy (AFM). Moreover, water contact angle and porosity tests were conducted. The influence of FeTCNPs on membranes fouling was evaluated using bovine serum albumin (BSA) as a model foulant.

2. Experimental

2.1. Materials

PES (Ultrason E6020P) obtained from BASF SE, Germany and *N,N*-DMF purchased from Avantor Performance Materials Poland S.A. were used for preparation of membrane casting solution, whereas pure water (Elix 3, Millipore) was used as a nonsolvent. Fe_3O_4 -trisodium citrate nanoparticles (FeTCNPs) were synthesized by chemical coprecipitation. All reagents used in FeTCNPs preparation, that is, $\text{FeCl}_3 \cdot 6\text{H}_2\text{O}$, $\text{FeSO}_4 \cdot 7\text{H}_2\text{O}$, NaOH, $\text{C}_6\text{H}_5\text{Na}_3\text{O}_7 \cdot 2\text{H}_2\text{O}$, and acetone were purchased from Avantor Performance Materials Poland S.A., Poland. BSA (Merck Millipore, Germany) in concentration of 1 g/L was applied as a model foulant.

2.2. Synthesis of FeTCNPs

FeTCNPs were prepared using chemical coprecipitation. Typically, 1.838 g of $\text{FeCl}_3 \cdot 6\text{H}_2\text{O}$ and 0.945 g of $\text{FeSO}_4 \cdot 7\text{H}_2\text{O}$ were dissolved in 150 mL of distilled water in a three-necked flask (500 mL). The obtained transparent solution was deaerated at nitrogen flow for 1 h. Thereafter, during rapid magnetic stirring, 20 mL of NaOH (10 M) was added into the solution within 30 min using a dropping funnel. After proceeded rapid stirring for 1 h, the resultant black dispersion was heated to 90°C and kept at this temperature for 1 h. After cooling to room temperature, the dispersion was subjected to magnetic separation with a magnet, and the collected magnetic mud was then redispersed in a 200 mL portion of trisodium citrate solution (0.3 M) and heated at 80°C for 1 h. The magnetic NPs were precipitated with acetone to remove the excessive citrate groups adsorbed on the nanomaterial, collected with a magnet, dried in an oven at 80°C, and next grinded using agate mortar.

The diameter of the obtained NPs assessed with the use of transmission electron microscopy (TEM) was in the range of 5–20 nm (Fig. 1).

2.3. Preparation of membranes

Both pure PES and PES/FeTCNPs membranes were prepared by the wet phase inversion method. The casting solution for fabrication of the unmodified membrane (M1) with polymer concentration of 15 wt% was obtained by dissolution of 8.38 g of PES in 50 mL of DMF. The homogeneous casting dope, after degassing, was casted onto a glass plate using automatic film applicator (Elcometer 4340, Elcometer Ltd., UK) with the knife gap of 0.1 mm and subsequently immersed in a pure water bath (20°C ± 1°C) for 24 h to complete the phase inversion process. The PES/FeTCNPs membranes (M2, M3, and M4) were fabricated by addition of 1, 2, or 4 wt% of FeTCNPs by weight of PES to previously prepared polymer solution (15 wt% PES in DMF). In order to

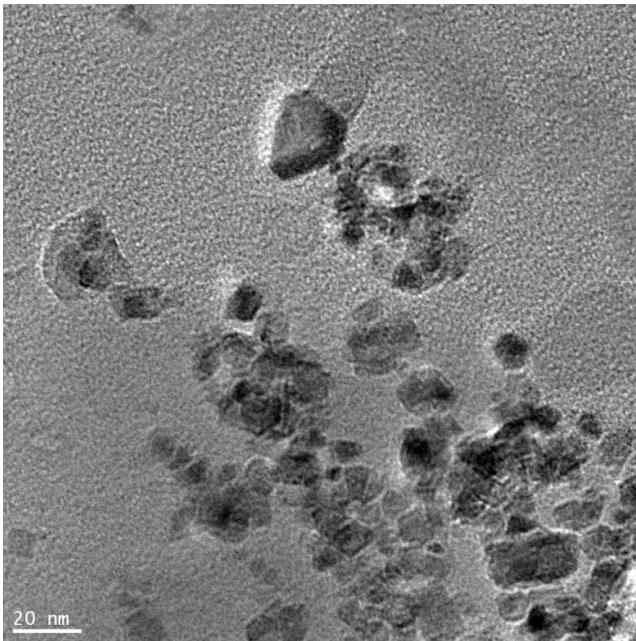


Fig. 1. TEM images of the prepared Fe₃O₄-trisodium citrate nanoparticles.

disperse FeTCNPs in a casting solution, a vigorous mechanical stirring was applied. After degassing, the membranes were casted using the automatic film applicator as described earlier.

2.4. Characterization of membranes

Hydrophilic properties of the prepared membranes were assessed based on water contact angle (θ) measurements performed with the use of a goniometer (Surface Energy Evaluation System, Advex Instruments, Czech Republic). The contact angle values were calculated as an average of at least five measurements from five different membrane pieces.

The porosity of membranes was determined using gravimetric analysis and calculated on a basis of the following equation:

$$P = \frac{(m_{\text{wet}} - m_{\text{dry}}) / \rho_w}{(m_{\text{wet}} - m_{\text{dry}}) / \rho_w + m_{\text{dry}} / \rho_p} \times 100\% \quad (1)$$

where m_{wet} and m_{dry} are weights (g) of membrane samples in the wet and the dry state, respectively; ρ_w is water density at 20°C ($\rho_w = 0.9982 \text{ g/cm}^3$), and ρ_p is the PES density (1.37 g/cm^3). The given values were obtained from three repeated measurements.

The topography of membranes surface was evaluated with the application of NanoScope V Multimode 8 scanning probe microscope (Bruker Corp., USA). The AFM measurements were performed with the silicon nitride ScanAsyst-Air probe in the ScanAsyst mode. The scanned area was $5 \mu\text{m} \times 5 \mu\text{m}$. Before analysis, the samples were soaked in water and ethanol solutions and air-dried to keep the surface unchanged.

Hitachi SU8020 Ultra-High Resolution Field Emission Scanning Electron Microscope (UHR FE-SEM) was applied for examination of membranes cross section. Before analysis, the samples previously dewatered in ethanol-water solutions were broken in liquid nitrogen and sputtered with a 5 nm thick chromium layer (Q150T ES coater, Quorum Technologies Ltd., UK). The images were collected in two modes of measurement: secondary electrons (SE, accelerating voltage: 5 kV) and backscattered electrons (BSE, 15 kV).

2.5. Membrane installation

The investigations were conducted in the laboratory scale installation presented in Fig. 2. The feed was pumped from the feed tank into a stainless steel membrane module using a peristaltic pump. The module was equipped with a manometer and a needle valve. The permeate flux was calculated based on the volume of the solution passing through the membrane during a fixed period of time. All experiments were repeated at least twice. For the determination of PWF the transmembrane pressure (TMP) was set at 0.05–0.15 MPa. The membrane fouling experiments with BSA solution were conducted at TMP = 0.1 MPa and the feed cross-flow velocity (CFV) of 0.8 m/s. The temperature was maintained at $20^\circ\text{C} \pm 1^\circ\text{C}$.

3. Results and discussion

3.1. Characterization of FeTCNPs nanocomposite membranes

Table 1 presents selected properties of the fabricated membranes. A slight increase of the porosity (69%–73%) with the increasing concentration of FeTCNPs (1–4 wt%) incorporated within a membrane matrix was observed. That can be explained in terms of the action of NPs, which are considered as pore forming agents [28]. In their work, Chen et al. prepared membranes containing in situ generated SiO₂ NPs. They proposed that upon generation, most of the SiO₂ NPs were trapped in the upper part of a membrane. Subsequently, a release of some of NPs could have occurred due to the physical incompatibilities between polymeric and inorganic

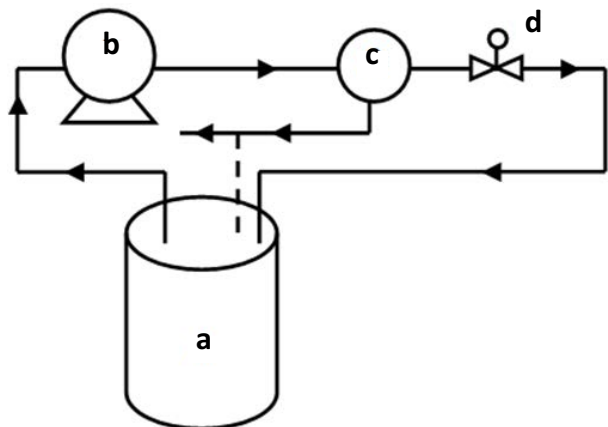


Fig. 2. The schematic diagram of the membrane installation used in the experiments (A – feed tank, B – peristaltic pump, C – membrane module, and D – needle valve with manometer).

Table 1
Selected properties of prepared membranes

Membrane	M1	M2	M3	M4
Porosity (%)	69	71	72	73
Contact angle (°)	57	55	54	58
Permeability (L/m ² h bar)	162	162	181	150

materials leading to a formation of a more loose skin layer of the membrane. Furthermore, since SiO₂ NPs exhibited high hydrophilicity, an enhanced transfer of the nanofiller from the skin layer to the coagulation bath could also take place. In such a case, the spaces previously occupied by the NPs would turn into membrane pores with a size related to the diameters of SiO₂ nanomaterial [28]. Similar explanation can be used in case of the results presented in Table 1.

Water contact angle is a parameter describing hydrophilicity of a membrane surface, and a decrease of contact angle indicates on an increase of hydrophilicity. Table 1 shows that after incorporation of FeTCNPs in the membrane structure, the changes in contact angle were not very significant. The value of this parameter in case of the neat membrane amounted to 57° and in case of the modified membranes it ranged from 54° to 58°, being the lowest for M3.

The transport properties of the fabricated membranes were evaluated based on water permeability (Table 1). The analysis of the results revealed that the modification with FeTCNPs had a noticeable influence on this parameter. In case of the membrane containing 2 wt% of the nanofiller (M3), the permeability increased for ca. 12% in comparison with the unmodified membrane (M1). When the lowest amount of NPs was used (M2 membrane), no effect of the modification on the permeate flux was observed. However, when the content of FeTCNPs within the membrane matrix was the highest (M4), the permeability decreased compared with the neat membrane by ca. 8%. The observed decrease can be explained in terms of the entrapment of poorly dispersed FeTCNPs in the membrane associated with a too high concentration of NPs [18] or surface pore blockage by the NPs agglomerates, discussed later. The M4 membrane also exhibited the highest contact angle, which could be another reason for the observed flux decline. In case of M2 and M3 membranes, a slight improvement of hydrophilicity was observed, which could contribute to the enhancement of water permeability through membrane pores.

SEM images of the cross-sections of the unmodified membrane and membranes modified with different concentrations of FeTCNPs are summarized in Fig. 4. The left column presents microphotographs collected in the SE mode, while in the right column the SEM-BSE images are shown. The membranes exhibited typically asymmetric structure with a dense top layer, a porous sublayer with relatively small finger-like pores, and a bottom layer consisting of fully developed macropores with finger- or bubble-like shapes. The formation of spongy structure in the sub- and bottom layer also occurred.

The analysis of cross-sections of modified membranes revealed the presence of large aggregates (ca. 6 μm) of FeTCNPs in case of M3 (Figs. 3(g) and (h)) and M4 (Figs. 3(k) and (l)), that is, ones containing the highest amount of the nanofiller. For these two membranes also much smaller and

well dispersed agglomerates were visible (Figs. 3(e) and (f) and (i) and (j)). The observation proved a nonhomogeneity of the structure of the mixed matrix membranes. However, despite this nonuniform distribution of NPs, the degree of dispersion was sufficient to contribute to an improvement of

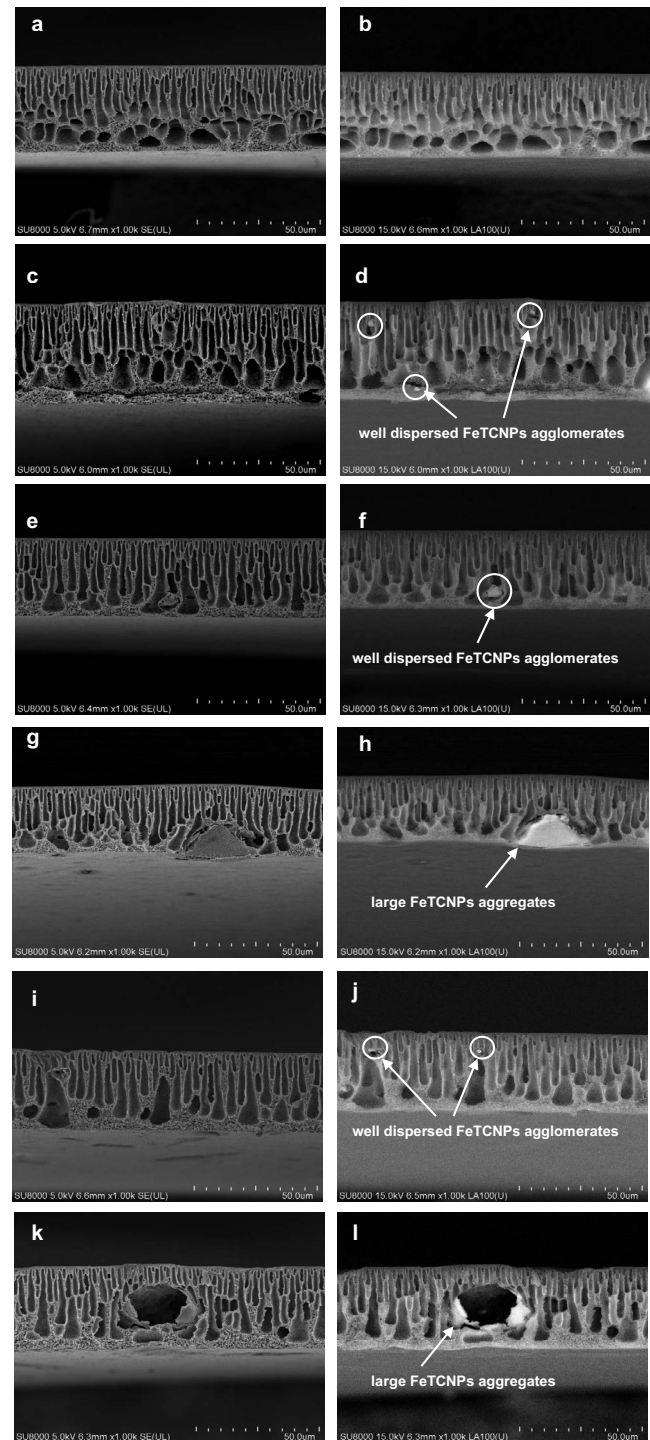


Fig. 3. SEM cross-section images of the unmodified membrane M1 ((a) and (b)) and membranes modified with different FeTCNPs concentration: M2 ((c) and (d)), M3 ((e)–(h)), M4 ((i)–(l)). The images on the right side ((b), (d), (f), (h), (j), and (l)) were collected in the BSE mode in order to highlight FeTCNPs incorporated within membrane matrix.

the permeate flux during UF of water in case of M3 membrane (Table 1). Nonetheless, in case of M4, the concentration of these large aggregates was too high, which resulted in a much larger number of formed hunks creating a barrier for water filtration and led to the lowest permeability among all studied membranes (Table 1). Furthermore, Figs. 3(k) and (l) confirm the postulate that at the stage of the membrane formation some NPs were removed from the polymer film and the spaces previously occupied by the NPs turned into membrane pores with a size related to the diameters of the nanomaterial. The SEM analysis of the membrane skin layer also proved this phenomenon. Based on the microphotographs shown in Fig. 4, the presence of large holes in the membrane surface was found. Some holes contained NPs that got stuck in the membrane (Fig. 4(a)), while in case of other ones NPs were not present (Fig. 4(b)). These “empty” imperfections were most probably formed as a result of destruction of the membrane top layer by large FeTCNPs aggregates, which were removed from the polymer film at the stage of the membrane formation, either during the immersion in the coagulation bath or, alternatively, during the casting of the dope onto glass plate. The pores with large diameters formed in this way could possibly increase the permeability, however, no increase of the PWF was observed in case of the M4 membrane (Table 1). A decrease of PWF was instead noted, which suggested that the presence of the holes presented in Fig. 4(b) was occasional, and the aggregates of NPs rather

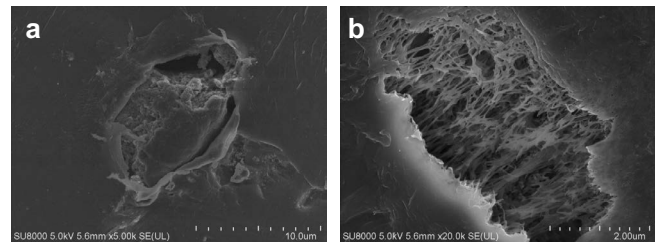


Fig. 4. SEM images of the M4 membrane surface (a) hole formed by large nanoparticles that got stuck in the membrane and (b) hole formed by large FeTCNP aggregate removed from the polymer film at the stage of membrane formation.

blocked the already formed pores, thus reduced the membrane permeability.

The changes of surface morphology of nanocomposite FeTCNPs/PES membranes and the unmodified M1 were also characterized by AFM analysis and 3D images are presented in Fig. 5. The unmodified membrane had a smooth surface (Fig. 5(a)), while in case of modified membranes the presence of NPs could be observed. On the surface of the membrane containing 4 wt% of FeTCNPs (M4), numerous irregular, large, and high (up to 400 nm) clusters of the nanomaterial were present, covering a large area of the skin (Fig. 5(d)). Membranes modified with lower amounts of FeTCNPs (M2 and M3) exhibited the presence of much smaller

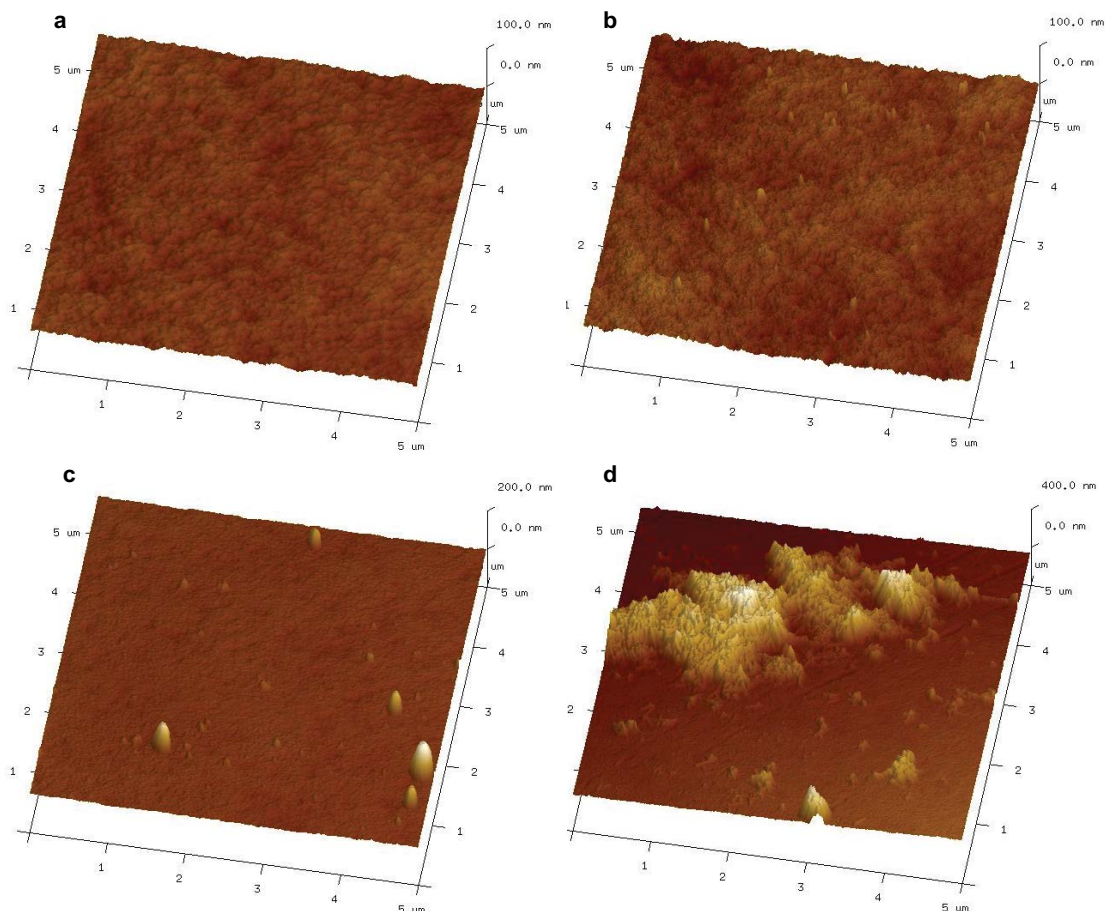


Fig. 5. AFM images of the unmodified M1 (a) and modified M2 (b), M3 (c), and M4 (d) membranes.

mountain-like agglomerates with height of ca. 50–200 nm (Figs. 5(b) and (c)). However, it should be stressed that the agglomerates, in case of the M2 membrane, were definitely smaller (Fig. 5(b)) than those observed for M3 membrane. The obtained results could confirm the slight changes in the surface hydrophilicity and PWF of the prepared membranes. The M4 membrane had numerous and very large aggregates of NPs on its surface, which blocked pores and thus reduced the water flow through the membrane resulting in a deterioration of its permeability. The topography of the surface of M1 and M2 was relatively similar and the number of NPs in case of M1 was very low, which explained the similar PWFs achieved for these membranes (Table 1). When the amount of NPs on the membrane surface increased (M3), but the aggregates and agglomerates were well dispersed, the hydrophilicity was the highest and the water permeability was significantly enhanced (Table 1).

3.2. Membrane fouling studies

In order to determine the influence of the applied modification on antifouling properties of the prepared membranes, the BSA solution of concentration of 1 g/L was applied as a model foulant. The change of normalized permeate fluxes measured during UF of BSA solution through the unmodified M1 membrane and modified membranes is summarized in Fig. 6.

No significant influence of the application of the FeTCNPs at the concentration of 1 and 2 wt% on the improvement of permeate flux during BSA UF was found, while in case of the highest amount of NPs (4 wt%), the flux decline was much more severe than in case of the unmodified M1 membrane. The observed intensification of the membrane fouling in the presence of M4 can be explained in terms of too high concentration of NPs, which affected the surface properties of the membrane. As it can be seen in Fig. 5, the surface of this membrane was densely covered with FeTCNPs. Comparing this parameter with the slightly increased value of contact angle (Table 1), it can be concluded that the reason for the observed significant flux decline during UF of BSA increased roughness of the surface and slightly decreased hydrophilicity compared with M1. It is commonly accepted that the increase of membrane hydrophilicity results in a better

fouling resistance since most organic foulants, including proteins such as BSA, exhibit hydrophobic nature [29,30]. Furthermore, the increase of surface roughness can significantly change the nature of the membrane, so that an enhanced deposition of organic molecules (e.g., BSA), various particles or bacteria can occur [31,32]. The deposition can take place especially between aggregates of the nanomaterial densely packed on the membrane surface (Fig. 5(d)). In opposite, at two lowest concentrations of NPs, the surface hydrophilicity was higher than that of M1 and the roughness due to the presence of FeTCNPs on the surface was much lower than in case of M4 (height of the NPs agglomerates: ca. 50–200 vs 400 nm, respectively). As a result, a less severe decline of permeate fluxes through M2 and M3 measured during UF of BSA compared with M1 was observed.

4. Conclusions

The investigations on nanocomposite UF PES membranes modified with FeTCNPs (1–4 wt%) were presented and discussed. The physicochemical characteristics and proneness of the fabricated membranes to fouling were examined.

The membrane containing 2 wt% of FeTCNPs (M3) exhibited ca. 12% higher pure water permeability in comparison with that measured for the unmodified membrane. It was attributed to the highest hydrophilicity of this membrane and a scattered distribution of NPs on its surface. In opposite, the membrane modified with 4 wt% of FeTCNPs (M4) was characterized by the lowest permeability, which was explained in terms of blockage of the membrane pores by the high amount of NPs deposited on the M4 surface associated with a slight increase of the water contact angle.

The permeate flux decline during UF of BSA solution was less severe in case of membranes modified with 1 and 2 wt% of FeTCNPs than in the absence of NPs in the membrane matrix. A significant decrease of the permeate flux in case of the membrane with the highest concentration of the nanofiller (M4) was attributed to the coverage of its surface with numerous large, irregular NPs agglomerates, which contributed to the enhanced deposition of BSA molecules.

The research revealed that incorporation of FeTCNPs within PES membrane matrix had a limited influence on the improvement of their hydrophilicity and water permeability as well as antifouling properties.

Acknowledgment

We would like to thank BASF (Germany) for providing PES samples.

Symbols

m_{dry}	—	Weight of dry membrane samples, g
m_{wet}	—	Weight of wet membrane samples, g
ρ_p	—	Polymer (PES) density, g/cm ³
ρ_w	—	Water density, g/cm ³

References

- [1] Z. Wang, H. Wang, J. Liu, Y. Zhang, Preparation and antifouling property of polyethersulfone ultrafiltration hybrid membrane containing halloysite nanotubes grafted with MPC via RATRP method, *Desalination*, 344 (2014) 313–320.

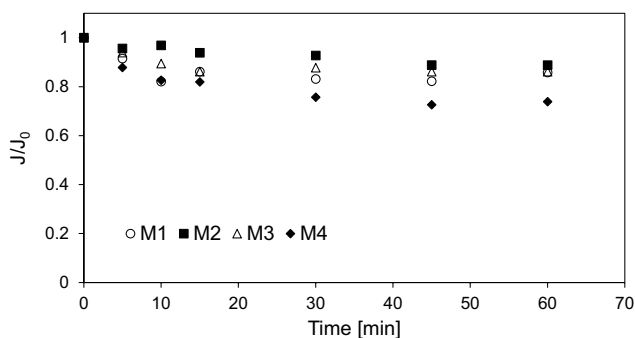


Fig. 6. The change of normalized permeate fluxes during ultrafiltration of BSA solution (1 g/L) through the unmodified (M1) and FeTCNPs-modified membranes (M2, M3, and M4). Process parameters: TMP = 0.1 MPa, CFV = 0.8 m/s.

- [2] H. Yu, X. Zhang, Y. Zhang, J. Liu, H. Zhang, Development of a hydrophilic PES ultrafiltration membrane containing SiO_2/N -Halamine nanoparticles with both organic antifouling and antibacterial properties, *Desalination*, 326 (2013) 69–76.
- [3] Y. Chen, Y. Zhang, J. Liu, H. Zhang, K. Wang, Preparation and antibacterial property of polyethersulfone ultrafiltration hybrid membrane containing halloysite nanotubes loaded with copper ions, *Chem. Eng. J.*, 210 (2012) 298–308.
- [4] N. Akar, B. Asar, N. Dizge, I. Koyuncu, Investigation of characterization and biofouling properties of PES membrane containing selenium and copper nanoparticles, *J. Membr. Sci.*, 437 (2013) 216–226.
- [5] W.Y. Wang, J.Y. Shi, J.L. Wang, J.L. Li, N.N. Gao, Z.X. Liu, W.T. Lian, Preparation and characterization of PEG-g-MWCNTs/PSf nano-hybrid membranes with hydrophilicity and antifouling properties, *RSC Adv.*, 5 (2015) 84746–84753.
- [6] J. Kim, B. Van der Bruggen, The use of nanoparticles in polymeric and ceramic membrane structures: review of manufacturing procedures and performance improvement for water treatment, *Environ. Pollut.*, 158 (2010) 2335–2349.
- [7] Z.Q. Huang, F. Zheng, Z. Zhang, H.T. Xu, K.M. Zhou, The performance of the PVDF- Fe_3O_4 ultrafiltration membrane and the effect of a parallel magnetic field used during the membrane formation, *Desalination*, 292 (2012) 64–72.
- [8] J. Alam, L.A. Dass, M. Ghasemi, M. Alhoshan, Synthesis and optimization of PES- Fe_3O_4 mixed matrix nanocomposite membrane: application studies in water purification, *Polym. Compos.*, 34 (2013) 1870–1877.
- [9] T. Agbaje, S. Al-Gharabli, M.O. Mavukkandy, J. Kujawa, H.A. Arafat, PVDF/magnetite blend membranes for enhanced flux and salt rejection in membrane distillation, *Desalination*, 436 (2018) 69–80.
- [10] M.M. Ba-Abbad, A.W. Mohammad, M.S. Takriff, R. Rohani, E. Mahmoudi, K.A. Faneer, A. Benamo, Synthesis of iron oxide nanoparticles to enhance polysulfone ultrafiltration membrane performance for salt rejection, *Chem. Eng. Trans.*, 56 (2017) 1699–1704.
- [11] M. Homayoonfal, M.R. Mehrnia, M. Shariaty-Niassar, A. Akbari, A.F. Ismail, T. Matsuura, A comparison between blending and surface deposition methods for the preparation of iron oxide/polysulfone nanocomposite membranes, *Desalination*, 354 (2014) 125–142.
- [12] M. Mukherjee, S. De, Reduction of microbial contamination from drinking water using an iron oxide nanoparticle impregnated ultrafiltration mixed matrix membrane: preparation, characterization and antimicrobial properties, *Environ. Sci. Water Res. Technol.*, 1 (2015) 204–217.
- [13] M. Mukherjee, S. De, Investigation of antifouling and disinfection potential of chitosan coated iron oxide-PAN hollow fiber membrane using gram-positive and gram-negative bacteria, *Mater. Sci. Eng., C*, 75 (2017) 133–148.
- [14] M. Mukherjee, S.R. Panda, S. De, Adhesion resistant chitosan coated iron oxide polyacrylonitrile mixed matrix membrane for disinfection of surface water, *J. Chem. Technol. Biotechnol.*, 92 (2017) 408–419.
- [15] A. Gholami, A.R. Moghadassi, S.M. Hosseini, S. Shabani, F. Gholami, Preparation and characterization of polyvinyl chloride based nanocomposite nanofiltration-membrane modified by iron oxide nanoparticles for lead removal from water, *J. Ind. Eng. Chem.*, 20 (2014) 1517–1522.
- [16] N. Abdullah, R.J. Gohari, N. Yusof, A.F. Ismail, J. Juhana, W.J. Lau, T. Matsuura, Polysulfone/hydrous ferric oxide ultrafiltration mixed matrix membrane: preparation, characterization and its adsorptive removal of lead (II) from aqueous solution, *Chem. Eng. J.*, 289 (2016) 28–37.
- [17] N. Ghaemi, S.S. Madaeni, P. Daraei, H. Rajabi, S. Zinadini, A. Alizadeh, R. Heydari, M. Beygzadeh, S. Ghouzivad, Polyethersulfone membrane enhanced with iron oxide nanoparticles for copper removal from water: application of new functionalized Fe_3O_4 nanoparticles, *Chem. Eng. J.*, 263 (2015) 101–112.
- [18] P. Daraei, S.S. Madaeni, N. Ghaemi, E. Salehi, M. Khadivi, R. Moradian, B. Astinchap, Novel polyethersulfone nanocomposite membrane prepared by PANI/ Fe_3O_4 nanoparticles with enhanced performance for Cu(II) removal from water, *J. Membr. Sci.*, 415–416 (2012) 250–259.
- [19] K.H. Chan, E.T. Wong, A. Idris, N.M. Yusof, Modification of PES membrane by PEG-coated cobalt doped iron oxide for improved Cu(II) removal, *J. Ind. Eng. Chem.*, 27 (2015) 283–290.
- [20] K.H. Chan, E.T. Wong, M. Irfan, A. Idris, N.M. Yusof, Enhanced Cu(II) rejection and fouling reduction through fabrication of PEG-PES nanocomposite ultrafiltration membrane with PEG-coated cobalt doped iron oxide nanoparticle, *J. Taiwan Inst. Chem. Eng.*, 47 (2015) 50–58.
- [21] M. Mondal, M. Dutta, S. De, A novel ultrafiltration grade nickel iron oxide doped hollow fiber mixed matrix membrane: spinning, characterization and application in heavy metal removal, *Sep. Purif. Technol.*, 188 (2017) 155–166.
- [22] R. Krishnamoorthy, V. Sagadevan, Polyethylene glycol and iron oxide nanoparticles blended polyethersulfone ultrafiltration membrane for enhanced performance in dye removal studies, *e-Polym.*, 15 (2015) 151–159.
- [23] M. Sharma, G. Madras, S. Bose, PVDF membranes containing hybrid nanoparticles for adsorbing cationic dyes: physical insights and mechanism, *Mater. Res. Express*, 3 (2016) 1–14.
- [24] M. Noormohamadi, M. Homayoonfal, M.R. Mehrnia, F. Davar, Synergistic effect of concurrent presence of zirconium oxide and iron oxide in the form of core-shell nanoparticles on the performance of $\text{Fe}_3\text{O}_4/\text{ZrO}_2/\text{PAN}$ nanocomposite membrane, *Ceram. Int.*, 43 (2017) 17174–17185.
- [25] E. Demirel, B. Zhang, M. Papakyriakou, S. Xia, Y. Chen, Fe_2O_3 nanocomposite PVC membrane with enhanced properties and separation performance, *J. Membr. Sci.*, 529 (2017) 170–184.
- [26] M. Nemati, S.M. Hosseini, Fabrication and electrochemical property modification of mixed matrix heterogeneous cation exchange membranes filled with $\text{Fe}_3\text{O}_4/\text{PAA}$ core-shell nanoparticles, *Ionics*, 22 (2016) 899–909.
- [27] A.S. Hobaib, K.M. Sheetan, L. El Mir, Effect of iron oxide nanoparticles on the performance of polyamide membrane for ground water purification, *Mater. Sci. Semicond. Process.*, 42 (2016) 107–110.
- [28] W. Chen, Y. Su, L. Zhang, Q. Shi, J. Peng, Z. Jiang, In situ generated silica nanoparticles as pore-forming agent for enhanced permeability of cellulose acetate membranes, *J. Membr. Sci.*, 348 (2010) 75–83.
- [29] L. Wang, R. Miao, X. Wang, Y. Lv, X. Meng, Y. Yang, D. Huang, L. Feng, Z. Liu, K. Ju, Fouling behavior of typical organic foulants in polyvinylidene fluoride ultrafiltration membranes: characterization from microforces, *Environ. Sci. Technol.*, 47 (2013) 3708–3714.
- [30] M. Fonouni, R. Yegani, S. Anarjani, A. Tavakoli, Anti-fouling behaviors of surface functionalized high density polyethylene membrane in microfiltration of bovine serum albumin protein, *Polyolefins J.*, 4 (2017) 13–26.
- [31] A. Ahmad, A. Abdulkarim, S. Ismail, B. Ooi, Preparation and characterisation of PES-ZnO mixed matrix membranes for humic acid removal, *Desal. Wat. Treat.*, 54 (2015) 3257–3268.
- [32] E. Preedy, S. Perni, D. Nipič, K. Bohinc, P. Prokopovich, Surface roughness mediated adhesion forces between borosilicate glass and Gram-positive bacteria, *Langmuir*, 30 (2014) 9466–9476.